

# Advanced Column-IV Epitaxial Materials for Silicon-Based Optoelectronics

James C. Sturm

## Introduction

Over the past decade or so, research in silicon-based heterostructures has evolved from a few seminal publications on the growth and physical properties of  $\text{Si}_{1-x}\text{Ge}_x$  heteroepitaxial layers<sup>1-4</sup> to a technology currently entering large-scale commercial production for heterojunction bipolar transistors (HBTs).<sup>5</sup> During this period, extensive work has taken place on the optoelectronic applications of Si/ $\text{Si}_{1-x}\text{Ge}_x$ , such as 1.3–1.55- $\mu\text{m}$  detectors for optical communication,<sup>6,7</sup> 2–12- $\mu\text{m}$  infrared detectors for two-dimensional (2D) focal plane arrays for night vision and thermal imaging,<sup>8,9</sup> and infrared emitters for chip-to-chip optical communication<sup>10,11</sup> as well as waveguiding<sup>12</sup> and modulators. The overall goal of this work has been to merge optoelectronic functionality with the very large-scale integration and electronic signal processing capabilities of silicon to create a silicon-based "superchip."<sup>13-15</sup>

Since the mid-1980s, several inherent limitations of the Si/Ge material system for future heterojunction optoelectronic and more advanced electronic devices have become apparent. In this article, we review the work on the  $\text{Si}_{1-x}\text{Ge}_x\text{C}_y$  ternary alloys and  $\text{Si}_{1-x}\text{C}_y$  binary alloy material systems that have emerged over the past five years or so and address how they allow us to overcome these longstanding basic materials limitations of the  $\text{Si}_{1-x}\text{Ge}_x$  system. We also will briefly discuss the more recent  $\text{Sn}_x\text{Ge}_{1-x}$  material system.

## Limitations of the Si/Ge Materials System

Pseudomorphic  $\text{Si}_{1-x}\text{Ge}_x$  layers on Si(100) substrates have several very fortu-

itous properties that have enabled the rapid progress toward HBT commercialization. These include miscibility of Si and Ge over the complete alloy range, ease of growth at low temperature with near-atomic-level precision, bandgaps up to several hundred meV less than that of Si, and similar ease of doping in Si and  $\text{Si}_{1-x}\text{Ge}_x$ . However over the past decade, the field as a whole has been constrained by several significant limitations. The first of these is the well-known critical thickness for thermal stability against misfit dislocation formation due to the lattice mismatch. For a Ge fraction  $x$  of 0.2 and resulting bandgap change of ~150 meV, the critical thickness is only ~15 nm.<sup>16</sup> This, for example, severely limits the quantum efficiency of normal incidence detectors relying on excitation across the bandgap of  $\text{Si}_{1-x}\text{Ge}_x$ .

Second for structures grown commensurate on Si(100) substrates, the conduction-band offset is negligibly small, at least for Ge fractions less than 0.7.<sup>17</sup> This issue can be addressed by growing  $\text{Si}_{1-x}\text{Ge}_x$  relaxed buffers on top of the silicon substrate and then growing a pseudomorphic heterostructure (with a lateral lattice constant larger than that of Si) on top of the buffer.<sup>18,19</sup> Despite much work, such relaxed buffers still suffer from threading dislocation densities of the order of  $10^4$ – $10^5$   $\text{cm}^{-2}$ , making future large-scale applications uncertain.

Third the practical implementation of heterojunction device structures usually requires the placement of dopant atoms with respect to the heterojunctions using nanometer precision. Whereas this can be achieved during the initial growth of the heterostructure at temperatures of

700°C or below, such precision (and device performance) is often degraded from dopant diffusion during subsequent thermal processing during device fabrication.<sup>20,21</sup>

Finally  $\text{Si}_{1-x}\text{Ge}_x$  under all combinations of strain is an indirect-bandgap material, resulting in inefficient detection and emission of light based on processes involving transitions across the bandgap. There have been many attempts to create a direct-gap material by the "zone-folding" principle in short-period Si/Ge superlattices,<sup>22</sup> but such experiments have been inconclusive.

## $\text{Si}_{1-x}\text{C}_y$ and $\text{Si}_{1-x-y}\text{Ge}_x\text{C}_y$ Materials Growth and Structural Properties

In the early 1990s, several groups began very basic work investigating the addition of substitutional C to Si and  $\text{Si}_{1-x}\text{Ge}_x$  structures to extend the capabilities of Si-based heterojunctions beyond the boundaries imposed by the four limitations discussed in the previous section. The properties of the resulting materials were generally not known *a priori*, but these materials have now been found to have a set of fortuitous properties for overcoming most of the limitations of the Si/Ge materials system. Carbon has a very low solid solubility in Si ( $<10^{-4}$  at all temperatures). However early work demonstrated that, by using low-temperature (400–650°C) growth, it was possible to incorporate a few percent of substitutional carbon to create metastable layers of  $\text{Si}_{1-x-y}\text{Ge}_x\text{C}_y$  and  $\text{Si}_{1-x}\text{C}_y$ . The growth techniques used included remote plasma-enhanced chemical vapor deposition (CVD),<sup>23</sup> molecular-beam epitaxy (MBE),<sup>24,25</sup> and thermal<sup>26</sup> or rapid thermal CVD.<sup>27</sup> Typically carbon filaments were used as carbon sources for MBE and methylsilane or hydrocarbons for CVD. Substitutional carbon levels were of the order of 1% in early work and are currently on the level of 3–5%. The early work all demonstrated the ability to adjust the strain in pseudomorphic layers because of the small size of the carbon atom, which compensates for the strain introduced by 8–10 Ge atoms. For example,  $\text{Si}_{1-x}\text{C}_y$  layers on Si(100) were shown to be under tensile strain, and  $\text{Si}_{1-x-y}\text{Ge}_x\text{C}_y$  on Si(100) had reduced compressive strain for low C levels (compared to  $\text{Si}_{1-x}\text{Ge}_x$ ) (Figure 1<sup>25</sup>), and had zero strain or even tensile strain for higher carbon levels. Because of the reduction in strain as carbon is added to compressively strained  $\text{Si}_{1-x-y}\text{Ge}_x\text{C}_y$  on Si(100), the early work successfully showed an increase in the critical thickness as C was added.<sup>27</sup>

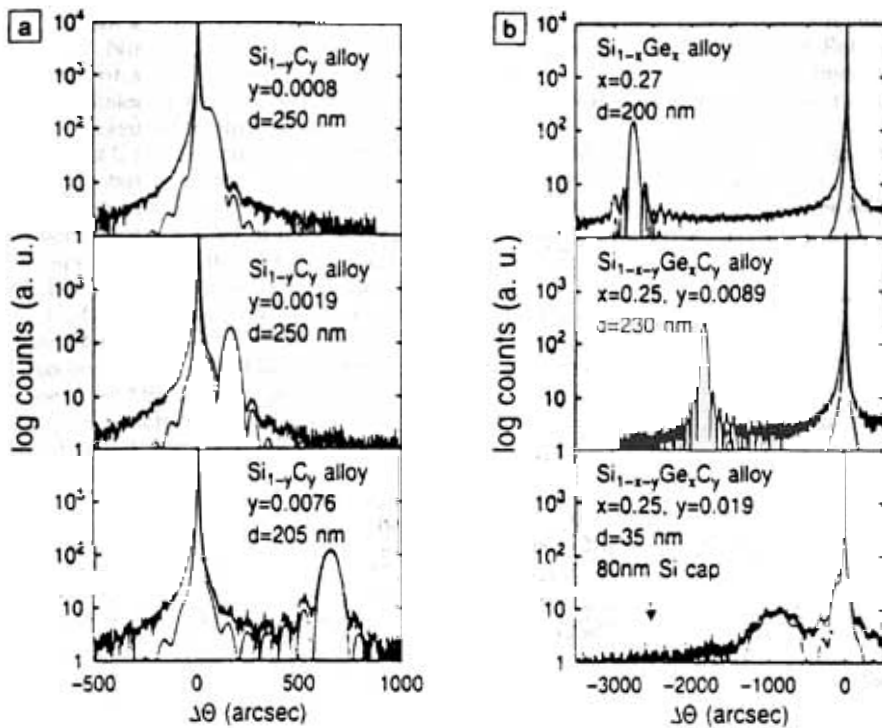


Figure 1. X-ray rocking curves of pseudomorphic (a)  $\text{Si}_{1-y}\text{C}_y$  and (b)  $\text{Si}_{1-x}\text{Ge}_x\text{C}_y$  of thickness  $d$ , grown on  $\text{Si}(100)$ . The images show the reduction of lattice constant as C is added, as well as simulations.<sup>25</sup> The arrow in (b) shows the peak of a pseudomorphic  $\text{Si}_{0.75}\text{Ge}_{0.25}$  layer without carbon. The tall peak in all curves is diffraction from the Si substrate.

The small size of the carbon atom introduces severe distortions in the lattice near carbon sites,<sup>28</sup> which can lead to new phases<sup>29</sup> and which affect the electronic structure.<sup>30</sup> A thorough review of such effects and early growth experiments exists.<sup>31</sup> Carbon can occupy an interstitial site in a Si (or  $\text{Si}_{1-x}\text{Ge}_x$ ) lattice as well as occupy a substitutional site. Above some limit, which strongly depends on growth conditions however, the carbon no longer incorporates substitutionally but instead incorporates interstitially. Because they may lead to deep levels, such interstitials may not be desirable. Figure 2 from Reference 32 presents an example of how varying growth conditions in CVD can affect the maximum substitutional levels of carbon, which can vary from as low as 0.3% to as high as 1.8% for the growth conditions of their studies. High-temperature annealing leads to SiC precipitates because of the low solubility of the carbon. This occurs mostly above 900°C,<sup>33</sup> so that there is optimism that practical device processing may be performed at lower temperatures without excessive degradation of the material quality. An especially im-

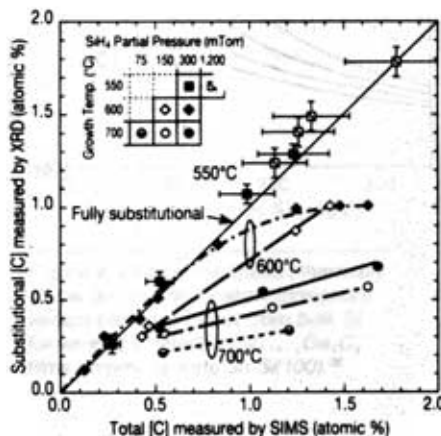


Figure 2. Dependence of substitutional carbon content upon chemical-vapor-deposition growth condition in  $\text{Si}_{1-y}\text{C}_y$  layers. Low-growth temperatures lead to higher substitutional levels.<sup>32</sup>

portant area of work in the next few years will be to attempt a better understanding of interstitial versus substitutional carbon and the affects of thermal

treatments and processing, especially below 900°C.

### Bandgap Effects

It was initially not known if carbon would lead to an increase or decrease in the bandgap of  $\text{Si}_{1-y}\text{C}_y$  or  $\text{Si}_{1-x-y}\text{Ge}_x\text{C}_y$  films. In relaxed films without strain, one might expect a large bandgap because of the large bandgap of SiC or diamond.<sup>34</sup> However the large lattice distortions near C sites have been predicted to lead to a lower bandgap and even a semimetal.<sup>35</sup> Photoluminescence measurements of compressively strained  $\text{Si}_{1-x-y}\text{Ge}_x\text{C}_y$  films with low C (<1%) and low Ge (<40%) showed an increase in the bandgap of +21–25 meV/%C.<sup>35,36</sup> The band edge is defined by the heavy hole band in the  $\text{Si}_{1-x-y}\text{Ge}_x\text{C}_y$  and four-conduction-band minima lying in  $k$ -space in a plane perpendicular to the growth direction. Transport measurements in HBTs with  $\text{Si}_{1-x-y}\text{Ge}_x\text{C}_y$  bases yielded a similar number, implying a uniform gap through the material.<sup>37</sup> Whereas the bandgap increases as carbon is added and the strain is reduced, the bandgap does not go up nearly as fast as it would if the strain were reduced solely by reducing the Ge fraction (Figure 3). Therefore for a given bandgap, the  $\text{Si}_{1-x-y}\text{Ge}_x\text{C}_y$  would have a lower strain and hence a higher critical thickness than a  $\text{Si}_{1-x}\text{Ge}_x$  layer of the same bandgap. The expected magnitude of this effect appears in Figure 4<sup>38</sup> which shows how the critical thickness of a  $\text{Si}_{1-x-y}\text{Ge}_x\text{C}_y$  layer would shift as C is added, assuming similar elastic constants for  $\text{Si}_{1-x-y}\text{Ge}_x\text{C}_y$  and  $\text{Si}_{1-x}\text{Ge}_x$ . For example, for a layer with a target bandgap 100-meV less than Si, with no C the critical thickness (of  $\text{Si}_{0.86}\text{Ge}_{0.14}$ ) would be ~25 nm. With 1% C ( $\text{Si}_{0.82}\text{Ge}_{0.17}\text{C}_{0.01}$ ), the critical thickness would be ~70 nm. With 2% C ( $\text{Si}_{0.77}\text{Ge}_{0.21}\text{C}_{0.02}$ ), it would be over 1 μm as the strain were reduced to near zero. This demonstrates that  $\text{Si}_{1-x-y}\text{Ge}_x\text{C}_y$  alloy layers with small amounts of carbon offer a route to overcome the long-standing tradeoff of critical thickness versus bandgap offset from silicon that has limited the silicon-based heterojunction field since its inception.

As C is added to the compressively strained  $\text{Si}_{1-x-y}\text{Ge}_x\text{C}_y$  films, the strain is reduced. This by itself will cause the bandgap to increase. If one assumes deformation potentials of  $\text{Si}_{1-x-y}\text{Ge}_x\text{C}_y$  similar to those of  $\text{Si}_{1-x}\text{Ge}_x$ , from the above data one expects the bandgap of an unstrained alloy to decrease by ~20 meV/%C for initial amounts of carbon. This would imply a "bowing" of the curve of bandgap versus lattice constant<sup>36</sup> as

commonly occurs in between III-V compounds with a large difference in lattice constant. Note added in proof: The bandgap of such strain-free SiGeC (without dislocations) has recently been directly measured by luminescence, and the effect of C (apart from that of Ge) is to reduce the bandgap by  $-27 \text{ meV}/\%C$ .<sup>55</sup> The bandgap of  $\text{Si}_{1-x-y}\text{Ge}_x\text{C}_y$  alloys has also been measured by optical absorption, especially in films of high Ge content. For relaxed (heavily dislocated)  $\text{Ge}_{1-y}\text{C}_y$  films with up to 3% C, an increase of bandgap with C of  $50\text{--}100 \text{ meV}/\%C$  has been observed.<sup>59</sup> This discrepancy may be caused by different physical properties of Ge-rich films, a fundamental difference between absorption and luminescence/transport experiments or defect effects in the Ge-rich film.

The bandgap of  $\text{Si}_{1-y}\text{C}_y$  on Si(100) has been measured by photoluminescence,<sup>40</sup> and an elegant technique of photoluminescence under uniaxial stress has been used to confirm a type-I band alignment with respect to Si<sup>41</sup> as shown in Figure 5. The band-edge transitions in the  $\text{Si}_{1-y}\text{C}_y$  are between the light hole and the  $\Delta_2$  valleys in the conduction band (parallel to the growth direction). Because of the strong effect of the tensile strain in the  $\text{Si}_{1-y}\text{C}_y$ , the bandgap decreases sharply as initial levels of C are added ( $-65 \text{ meV}/\%C$ ). The bandgap decrease is larger than that expected from the strain alone ( $-46 \text{ meV}/\%C$ ) so that one finds that the effect of the C on a relaxed alloy would be expected to be  $-19 \text{ meV}/\%C$ . This is consistent with the value found for the effect of C on the inferred bandgap of relaxed  $\text{Si}_{1-x-y}\text{Ge}_x\text{C}_y$  films described earlier.

### Band Offsets

Beside the bandgap itself, how the conduction and valence bands align themselves across a heterojunction interface is of first-order importance for device applications. As mentioned earlier, there is little conduction-band offset in the  $\text{Si}_{1-x}\text{Ge}_x/\text{Si}$  material system if relaxed  $\text{Si}_{1-x}\text{Ge}_x$  buffers are not used. In compressively strained  $\text{Si}_{1-x-y}\text{Ge}_x\text{C}_y$  on Si(100), the valence-band offset to Si has been measured by capacitance-voltage (C-V) techniques on unipolar  $p^+ \text{Si}_{1-x-y}\text{Ge}_x\text{C}_y/p^- \text{Si}$  diodes and has been found to decrease at  $\sim 20\text{--}26 \text{ meV}/\%C$ ,<sup>38</sup> essentially the same rate at which the bandgap increases. This implies the band positions of  $\text{Si}_{1-x}\text{Ge}_x$  and  $\text{Si}_{1-x-y}\text{Ge}_x\text{C}_y$  with identical bandgaps to be nearly the same, so that no conduction-band offset of  $\text{Si}_{1-x-y}\text{Ge}_x\text{C}_y$  to a silicon (100) substrate is expected (Figure 5). This absence of a conduction-band offset and a similar va-

lence-band offset has also been confirmed by a metal-oxide-semiconductor C-V technique similar to that of Reference 42 and other methods.<sup>43</sup> There is not universal agreement on this topic however.<sup>44</sup>

A more fortuitous situation arises in the case of a tensile-strained  $\text{Si}_{1-y}\text{C}_y$  layer grown commensurate on a Si(100)

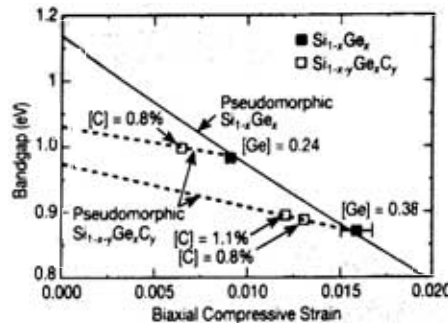


Figure 3. Bandgap for pseudomorphic  $\text{Si}_{1-x-y}\text{Ge}_x\text{C}_y$  and  $\text{Si}_{1-x}\text{Ge}_x$  on Si(100) as a function of compressive strain. For a similar bandgap,  $\text{Si}_{1-x-y}\text{Ge}_x\text{C}_y$  layers have lower strain.<sup>36</sup>

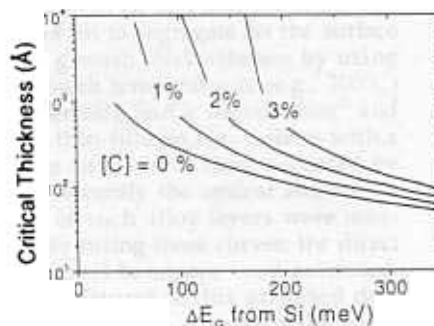


Figure 4. Critical thickness (thermally stable without dislocation formation) versus bandgap offset from bulk Si for various C levels in  $\text{Si}_{1-x-y}\text{Ge}_x\text{C}_y$  films commensurate on Si(100).<sup>38</sup>

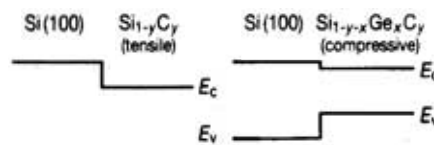


Figure 5. Qualitative picture of band-gap offsets of pseudomorphic  $\text{Si}_{1-y}\text{C}_y$  (tensile strain) and  $\text{Si}_{1-x-y}\text{Ge}_x\text{C}_y$  (compressive strain) on Si(100).

substrate. As in the case of tensile-strained Si on a relaxed  $\text{Si}_{1-x}\text{Ge}_x$  "substrate," the strain leads to a substantial splitting of the conduction band with electrons being confined to the film under tensile strain. This offset has been measured by both C-V techniques<sup>42</sup> and by the successful fabrication of 2D electron gases with the electrons confined to the  $\text{Si}_{1-y}\text{C}_y$  layer.<sup>45</sup> The offset is  $75\text{--}90 \text{ meV}/\%C$  with the conduction band lying lower in the  $\text{Si}_{1-y}\text{C}_y$  (Figure 5). This offset is more than sufficient with  $1\text{--}2\% C$  to make well-defined 2D electron gases through the modulation-doping technique.<sup>45</sup> It is not yet known however if the presence of C will lead to substantial alloy scattering and severely limit the mobility of these layers.

### Effect of Carbon on Diffusion in Si-Based Heterostructures

We have shown that  $\text{Si}_{1-x-y}\text{Ge}_x\text{C}_y$  and  $\text{Si}_{1-y}\text{C}_y$  alloys allow one to overcome two long-standing fundamental limitations to the Si-based heterojunction field—critical thicknesses and the lack of a significant conduction-band offset for structures pseudomorphic to Si(100) substrates. In practice the problem of dopant diffusion during processing can severely limit the utility of most Si-based heterojunction devices. This is because many desired devices (e.g., a high-mobility electron gas using modulation doping) require the dopant be placed using nm-precision with respect to the heterojunction, and the dopant can diffuse during subsequent thermal processing after growth. Unfortunately some thermal processing is nearly inevitable during the integration of devices onto silicon-integrated circuits, and integration is one of the overriding goals of the field. In the past few years, however, it has emerged that small amounts of substitutional C can lead to a dramatic reduction in the amounts of boron diffusion, especially when resulting from interstitial injection mechanisms such as oxidation or implant annealing. This mechanism appears to be similar in either carbon-doped silicon<sup>46</sup> or  $\text{Si}_{1-x-y}\text{Ge}_x\text{C}_y$  films. Significant effects can already occur for C levels as low as  $10^{19} \text{ cm}^{-3}$ . An example of how the enhanced diffusion due to overlying ion implant damage of a buried boron layer can be suppressed by substitutional C appears in Figure 6. This figure shows the base profile of the boron and Ge in a  $\text{Si}_{1-x-y}\text{Ge}_x\text{C}_y$ -base HBT after the top 50 nm (far from the boron) were subjected to an  $\text{As}^+$  ion implant of dose  $1.8 \times 10^{15} \text{ cm}^{-2}$ , followed by 10-min annealing at  $755^\circ\text{C}$ . Note the presence of significant boron



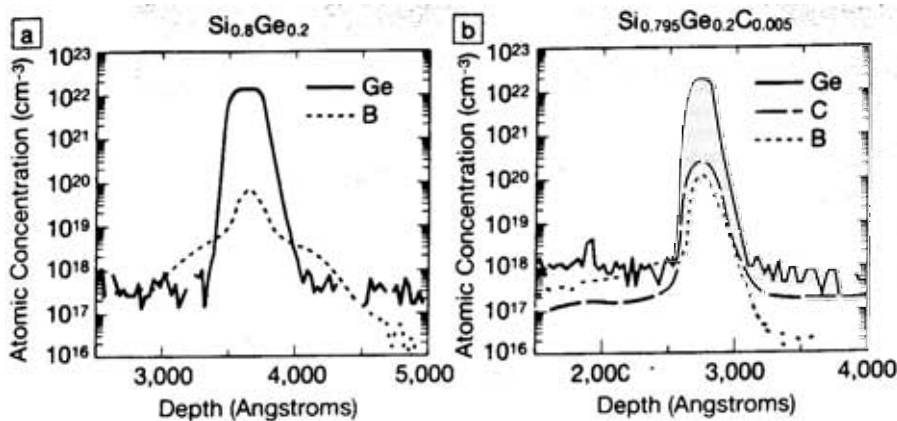


Figure 6. Comparison of boron profiles (from secondary ion mass spectrometry) in  $\text{Si}_{1-x}\text{Ge}_x$ -based and  $\text{Si}_{1-x}\text{Ge}_x\text{C}_y$ -based heterojunction bipolar transistors after ion implantation of the top surface (50 nm) with  $\text{As}^-$  of dose  $1.8 \times 10^{15} \text{ cm}^{-2}$ , followed by 10-min annealing at  $755^\circ\text{C}$  in nitrogen.<sup>47</sup>

diffusion in the sample without C (which had abrupt boron profiles before annealing) and the absence of such diffusion in the sample with 0.5% C. This reduced boron diffusion has been observed to give rise to a marked improvement in the HBT characteristics.<sup>47</sup>

Substitutional C acts as a sink for Si self-interstitials, which are known to be required for boron diffusion. However the exact complexes that form between the Si interstitials and the carbon and their quantitative relationship to boron diffusion are not yet known, and their effect on electronic properties is not known. The degree to which the  $\text{Si}_{1-x}\text{Ge}_x$  or  $\text{Si}_{1-x}\text{Ge}_x\text{C}_y$  can suppress boron diffusion in carbon-free regions outside the carbon-containing regions is also not known.<sup>47</sup> Nevertheless because boron diffusion is such a common issue in silicon-based device fabrication,  $\text{Si}_{1-x}\text{Ge}_x\text{C}_y$  and  $\text{Si}_{1-x}\text{C}_y$  layers may be very useful for properties other than their electronic structure or optical properties.

### Direct Bandgaps in Column-IV Materials

$\text{Si}_{1-x}\text{Ge}_x$ ,  $\text{Si}_{1-x}\text{C}_y$ , and  $\text{Si}_{1-x}\text{Ge}_x\text{C}_y$  alloys are all indirect-bandgap materials. "No-phonon" luminescence is regularly observed, but this is because alloy scattering due to the random nature of the alloy can be used to conserve momentum in transitions between the conduction and valence band.<sup>48-50,35,36,40</sup> Although stronger than the phonon-assisted processes, this is still a relatively weak process, making the fabrication of high-efficiency optical detectors and high-efficiency optical emitters inherently difficult.

The direct bandgap in Ge is only 0.1 eV above the indirect gap. It has long been recognized that an alloy of cubic tin and Ge might pull this direct gap below the indirect gap, leading to a direct-bandgap semiconductor consisting of all column-IV materials.<sup>51,52</sup> The growth of such layers is difficult because of the low solubility of Sn in Ge and because of the tendency of Sn to segregate on the surface during growth. Nevertheless by using low-growth temperatures (e.g.,  $200^\circ\text{C}$ ) and other aids, Sn/Ge superlattices<sup>53</sup> and relaxed thin-film  $\text{Sn}_x\text{Ge}_{1-x}$  alloys with  $x$  as large as 0.3 have been reported by MBE.<sup>54</sup> Recently the optical absorption curves of such alloy layers were measured. By fitting these curves, the direct and indirect bandgaps were extracted. The key features of this extracted data appear in Table I. Although the films suffered from significant subgap absorption, a transition from indirect to direct gap occurs for Sn concentrations between 0.11 and 0.15 eV. Although SnGe

work is still in its early stages, these results may be the first evidence of the formation of a direct-bandgap semiconductor of all column-IV materials and will open new possibilities for the creation of column-IV-based optoelectronics.

### Summary

Fundamental issues that have limited the development of optoelectronics in the Si/Ge material system have been discussed. These include the critical thickness issue, the lack of a conduction-band offset for layers commensurate on Si(100) substrates, the sensitivity of devices to dopant diffusion, and the lack of a direct bandgap. Recent results in the  $\text{Si}_{1-x}\text{C}_y$ ,  $\text{Si}_{1-x}\text{Ge}_x\text{C}_y$ , and  $\text{Sn}_x\text{Ge}_{1-x}$  materials systems show that materials solutions exist for all of these problems. Much more work remains both to exploit these new possibilities in devices and to solve outstanding materials issues. However for the first time, we have a basic set of materials with which to realize optoelectronic chips based on all column-IV materials.

### Acknowledgments

The assistance of C.L. Chang in the preparation of this manuscript is appreciated. The support of the Office of Naval Research, the U.S. Air Force Rome Laboratory, the National Science Foundation, and the von Humboldt Foundation is gratefully acknowledged.

### References

1. E. Kasper, H.J. Herzog, and H. Kibbel, *Appl. Phys.* **8** (1975) p. 199.
2. H.M. Manasevit, I.S. Gergis, and A.B. Jones, *J. Electron. Mater.* **12** (1983) p. 637.
3. J.C. Bean, T.T. Sheng, L.C. Feldman, A.T. Fiory, and R.T. Lynch, *Appl. Phys. Lett.* **44** (1984) p. 102.
4. R. People, *Phys. Rev. B* **32** (1985) p. 1405.
5. D.C. Ahlgren, M. Gilbert, D. Greenberg, S.-J. Jeng, J. Malinowski, D. Nguyen-Ngoc, K. Schonenberg, K. Stein, R. Groves, K. Walter, D. Sunderland, D.L. Harnane, and B. Meyerson,

Table I: Direct and Indirect Bandgaps of  $\text{Sn}_x\text{Ge}_{1-x}$  Alloys Extracted From Optical Absorption Measurements.<sup>54\*</sup>

$\text{Sn}_x\text{Ge}_{1-x}$ Composition	Absorption Feature	Energy (meV)
$x = 0.06$	Direct gap	614±4
	Indirect gap	599±19
$x = 0.11$	Direct gap	445±3
	Indirect gap	428±19
$x = 0.15$	Direct gap	346±3
	Indirect gap	441±4

\*A direct-bandgap material is found for  $x = 0.15$ .

Tech. Dig. Int. Electron Device Meeting (1996) p. 859.

6. S. Luryi, T.P. Pearsall, H. Temkin, and J.C. Bean, *IEEE Electron Device Lett.* 7 (1986) p. 104.  
7. A. Splett, T. Zinke, K. Petermann, E. Kasper, H. Kibbel, H.-J. Herzog, and H. Presting, *IEEE Photonics Tech. Lett.* 6 (1994) p. 59.  
8. T.L. Lin and J. Maserjian, *Appl. Phys. Lett.* 57 (1990) p. 1422.  
9. R.P.G. Karunasiri, J.S. Park, and K.L. Wang, *ibid.* 59 (1991) p. 2588.  
10. Q. Mi, X. Xiao, J.C. Sturm, L. Lenchyshyn, and M.L.W. Thewalt, *ibid.* 60 (1992) p. 3177.  
11. H. Presting, T. Zinke, A. Splett, H. Kibbel, and M. Jaros, *ibid.* 69 (1996) p. 2376.  
12. R. Soref, F. Namavar, and J.P. Lorenzo, *Proc. SPIE* 1177 (1989) p. 175.  
13. R. Soref, *Proc. IEEE* 81 (1993) p. 1687.  
14. G. Abstreiter, *Phys. World* (UK) 5 (1992) p. 36.  
15. D.C. Houghton, J-P. Noel, and N.L. Rowell, in *Silicon Molecular-Beam Epitaxy*, edited by J.C. Bean, S.S. Iyer, and K.L. Wang (Mater. Res. Soc. Symp. Proc. 220, Pittsburgh, 1991) p. 299.  
16. D.C. Houghton, C. Gibbings, C. Tuppen, M. Lyons, and M. Halliwell, *Appl. Phys. Lett.* 56 (1990) p. 460.  
17. C. Van de Walle, *Phys. Rev. B* 34 (1986) p. 5621.  
18. Y.J. Mii, Y.H. Xie, E.A. Fitzgerald, D. Monroe, F.A. Theil, B.E. Weir, and L.C. Feldman, *Appl. Phys. Lett.* 59 (1991) p. 1611.  
19. K. Ismail, S. Rishton, J.O. Chu, K. Chan, and B.S. Meyerson, *IEEE Electron Device Lett.* 14 (1993) p. 348.  
20. E.J. Prinz, P.M. Garone, P.V. Schwartz, X. Xiao, and J.C. Sturm, *ibid.* 12 (1991) p. 42.  
21. J.W. Slotboom, B. Streutker, A. Pruijboom, and D.J. Gravesteejn, *ibid.* p. 486.  
22. U. Gnutzmann and K. Clausecker, *Appl. Phys.* 3 (1974) p. 9.  
23. J.B. Posthill, R.A. Rudder, S.V. Hat-

tangaddy, C.G. Fountain, and R.J. Markunas, *Appl. Phys. Lett.* 56 (1990) p. 734.

24. S.S. Iyer, K. Eberl, F.K. LeGoues, J.C. Tsang, and F. Cardone, *ibid.* 60 (1992) p. 356.  
25. K. Eberl, S.S. Iyer, S. Zollner, J.C. Tsang, and F.K. LeGoues, *ibid.* p. 3033.  
26. M. Hiroi, K. Miyayaga, and T. Tatsumi, in *Ext. Abs. 1993 Conf. Solid State Dev. Mater.* (Japan Society of Applied Physics, Makuhari, 1993) p. 934.  
27. J.L. Regolini, F. Gisbert, G. Dolino, and P. Boucaud, *Mater. Lett.* 18 (1993) p. 57.  
28. B. Dietrich, H.J. Osten, H. Ruecker, M. Methfessel, and P. Zaumseil, *Phys. Rev. B* 49 (17) (1994) p. 185.  
29. H. Rueker, M. Methfessel, E. Bugiel, and H.J. Osten, *Phys. Rev. Lett.* 72 (1994) p. 3578.  
30. A.A. Demkov and O.F. Sankey, *Phys. Rev. B* 48 (1993) p. 227.  
31. S.C. Jain, H.J. Osten, B. Dietrich, and H. Ruecker, *Semicond. Sci. Technol.* 10 (1995) p. 1289.  
32. T.O. Mitchell, J.L. Hoyt, and J.F. Gibbons, *Appl. Phys. Lett.* 71 (1997) p. 1688.  
33. M.S. Goorsky, S.S. Iyer, K. Eberl, F. LeGoues, J. Angiello, and F. Cardone, *ibid.* 60 (1992) p. 32758.  
34. R.A. Soref, *J. Appl. Phys.* 70 (1991) p. 2470.  
35. P. Boucaud, C. Francis, F.H. Julien, J.-M. Lourtioz, D. Bouchier, S. Bodnar, B. Lambert, and J.L. Regolini, *Appl. Phys. Lett.* 64 (1994) p. 875.  
36. A.St. Amour, C.W. Liu, J.C. Sturm, Y. LaCroix, and M.L.W. Thewalt, *ibid.* 67 (1995) p. 3915.  
37. L.D. Lanzerotti, A. St. Amour, C.W. Liu, J.C. Sturm, J.K. Watanabe, and N.D. Theodore, *IEEE Electron Device Lett.* 17 (1997) p. 334.  
38. C.L. Chang, A. St. Amour, and J.C. Sturm, *Tech. Dig. Int. Electronic Device Meeting* (1996) p. 257; C.L. Chang, A. St. Amour, and J.C. Sturm, *Appl. Phys. Lett.* 70 (1997) p. 1557.  
39. J. Kolodzey, P.A. O'Neil, S. Zhang, B.

Orner, K. Roe, K. Unruh, C. Swann, M. Waite, and S.I. Shah, *ibid.* 67 (1995) p. 1865.

40. K. Brunner, K. Eberl, and W. Winter, *Phys. Rev. Lett.* 76 (1996) p. 303; K. Eberl, K. Brunner, and W. Winter, *Thin Solid Films* 194 (1997) p. 98.  
41. D.C. Houghton, G.C. Aers, N.L. Rowell, K. Brunner, W. Winter, and K. Eberl, *Phys. Rev. Lett.* 78 (1997) p. 2441.  
42. J. Hoyt, K. Rim, T.O. Mitchell, K. Rim, D.V. Singh, and J.F. Gibbons, *Tech. Dig. 7th Int. Symp. Silicon MBE* (Banff, Canada, 1997) p. 41.  
43. J. Hoyt (private communication).  
44. B.L. Stein, E.T. Yu, E.T. Croke, A.T. Hunter, T. Laursen, A.E. Bair, J.W. Mayer, and C.C. Ahn, *Appl. Phys. Lett.* 70 (1997) p. 3413.  
45. K.W. Faschinger, S. Zerlauth, G. Bauer, and L. Palmetshofer, *ibid.* 67 (1995) p. 3933.  
46. P.A. Stolck, D.J. Eaglesham, H.-J. Gossman, and J.M. Poate, *ibid.* 66 (1995) p. 1370.  
47. L.D. Lanzerotti, J.C. Sturm, E. Stach, R. Hull, T. Buyuklimanli, and C. Magee, *ibid.* 70 (1997) p. 3125.  
48. K. Terashima, M. Tajima, and T. Tatsumi, *ibid.* 57 (1990) p. 1925.  
49. J. Sturm, H. Manoharan, L. Lenchyshyn, M. Thewalt, N. Rowell, J.-P. Noel, and D. Houghton, *Phys. Rev. Lett.* 66 (1991) p. 1362.  
50. J. Weber and M. Alonso, *Phys. Rev. B* 40 (1989) p. 5683.  
51. D.W. Jenkins and J.D. Dow, *ibid.* 36 (1987) p. 7994.  
52. K.A. Mader, A. Baldereschi, and H. von Känel, *Solid State Commun.* 69 (1989) p. 1123.  
53. W. Wegscheider, J. Olajos, U. Menczgar, W. Dondl, and G. Abstreiter, *J. Cryst. Growth* 123 (1992) p. 75.  
54. G. He and H.A. Atwater, *Phys. Rev.* 79 (1997) p. 1937.  
55. O.G. Schmidt and K. Eberl, *Phys. Rev. Lett.* In press. □